

1st July 2004

Revised version 1st January 2005, re-revised version 10th March 2005. Accepted by Phys. Rev. D.

## A nucleon in a tiny box

Paulo F. Bedaque\*

*Lawrence-Berkeley Laboratory, Berkeley, CA 94720, USA*

Harald W. Griebhammer†

*Institut für Theoretische Physik (T39), Technische Universität München, D-85747 Garching, Germany*

Gautam Rupak‡

*Los Alamos National Laboratory, Los Alamos, NM 87545, USA*

We use Chiral Perturbation Theory to compute the nucleon mass-shift due to finite volume and temperature effects. Our results are valid up to next-to-leading order in the “ $\epsilon$ -régime” ( $mL \sim m\beta \ll 1$ ) as well as in the “ $p$ -régime” ( $mL \sim m\beta \gg 1$ ). Based on the two leading orders, we discuss the convergence of the expansion as a function of the lattice size and quark masses. This result can be used to extrapolate lattice results obtained from lattice sizes smaller than the pion cloud, avoiding the numerical simulation of physics under theoretical control. An extraction of the low-energy coefficient  $c_3$  of the chiral Lagrangean from lattice simulations at small volumes and a “magic” ratio  $\beta = 1.22262L$  might be possible.

Lattice QCD simulations are necessarily performed in finite boxes. Finite-size effects are controlled by the parameter  $mL$ , where  $L$  is the lattice size and  $m$  the mass of the lightest particle, in QCD, the pion. Physical results can be obtained in the limit  $mL \gg 1$ . As the pion masses achieved in simulations approach the physical value it becomes harder to fulfill this condition. However, most of the configurations in large lattices describe pions traveling at large distances of the order of  $L$ . Since the physics of these soft-pions is strongly constrained by chiral symmetry, strong theoretical control over them makes their numerical simulation unnecessary. One can thus obtain physical results by simulating in smaller lattices and using Chiral Perturbation Theory ( $\chi$ PT) or some other relevant effective theory to include the soft-pion physics cut off by the box size and extrapolate the results to the infinite volume limit. Another way to describe the same procedure gives added insight: The low-energy physics in the infinite and finite volume are described by the same effective theory with the same low-energy constants, since the values of these constants encapsulate short-distance physics that is not modified by finite-volume effects. The comparison of finite volume lattice results with the effective theory prediction allows one therefore to determine the value of some of the low energy constants. Those, in turn, can be used to determine physical observables in the infinite-volume limit. This general procedure has been carried out in the régime  $mL \gg 1$ , where standard  $\chi$ PT can be applied, to a variety of one nucleon observables, see e.g. [1]. However, it is for  $mL \ll 1$  (in the so-called  $\epsilon$ -régime [2]) that the programme described above is fully realized. For such small boxes, most of the pion cloud surrounding a baryon is excluded, and we are left with a bare nucleon. There are some modifications to the usual  $\chi$ PT power counting in this régime. The first and obvious one is that the momenta are quantized in units of  $2\pi/L$ . More importantly, the pion zero mode fluctuations are not suppressed, become non-perturbative and need to be treated exactly [2]. They reduce the value of the chiral condensate and make the chiral condensate disappear altogether in the chiral limit. This is to be expected since there is no chiral symmetry breaking at finite volumes. Recently, the  $\epsilon$ -régime in the meson sector and its relevance to lattice QCD have been assessed in a number of papers [3]. In the present work, we extend the idea to the one-baryon sector. Convergence in the baryonic sector is typically worse than in the mesonic sector, as it receives contributions at every order in  $p/(4\pi f)$ , unlike the meson sector case where the expansion parameter is  $(p/(4\pi f))^2$ . We address this issue by comparing the sizes of leading and next-to-leading order contributions in a calculation of the nucleon mass.

\* pfbedaque@lbl.gov

† hgrie@ph.tum.de

‡ grupak@lanl.gov

We consider one nucleon in a small box of size  $\beta \times L^3$  for  $2\pi/(4\pi f) \lesssim \beta, L \lesssim 2\pi/m$ , the “ $\epsilon$ -régime”.  $L$  is the size of the spatial directions,  $\beta$  the temporal extend of the box, namely the inverse temperature. In this régime,  $\chi$ PT is valid, except that the relative counting between  $p$  and  $m$  is changed. Instead of the usual counting  $1/L, 1/\beta \sim m \sim p$  ( $p$ -counting), we use  $1/L, 1/\beta \sim m_q \sim \sqrt{m} \sim \epsilon$ , hence the name “ $\epsilon$ -régime” [2]. For small boxes, the first non-zero pion mode has a momentum  $p = 2\pi/L \gtrsim \Delta$ , so we include the  $\Delta(1232)$  as explicit degree of freedom, counting, in the  $\epsilon$ -régime,  $\Delta \sim m \sim \epsilon^2$ .

### THE $\epsilon$ EXPANSION IN THE BARYON SECTOR

Low-energy properties ( $Q \sim 1/L, 1/\beta$ ) of the system are described by the effective Euclidean Lagrangean

$$\begin{aligned}
\mathcal{L} &= \mathcal{L}_\pi + \mathcal{L}_N + \mathcal{L}_\Delta, \\
\mathcal{L}_\pi &= f^2 \text{Tr} \mathcal{A}_\mu \mathcal{A}_\mu - \frac{Bf^2}{2} \text{Tr}(\xi_R^\dagger \mathcal{M} \xi_L + \xi_L^\dagger \mathcal{M}^\dagger \xi_R) + \dots, \\
\mathcal{L}_N &= N^\dagger D_0 N - g_A N^\dagger \vec{\sigma} \cdot \vec{A} N + N^\dagger \left[ -\frac{\vec{D}^2}{2M} + \frac{g_A}{2M} \{ \vec{\sigma} \cdot \vec{D}, \mathcal{A}_0 \} - 2Bc_1 \text{Tr}(\xi_R^\dagger \mathcal{M} \xi_L + \xi_L^\dagger \mathcal{M}^\dagger \xi_R) \right. \\
&\quad \left. + 4(c_2 - \frac{g_A^2}{8M}) \mathcal{A}_0^2 + 4c_3 \mathcal{A}_\mu \mathcal{A}_\mu - (c_4 + \frac{1}{4M}) 2i\epsilon^{ijk} \mathcal{A}_i \mathcal{A}_j \sigma^k + \dots \right] N, \\
\mathcal{L}_\Delta &= -\Delta^{\dagger iA} (D_0 + \Delta - \frac{\vec{D}^2}{2M}) \Delta^{iA} + g_{N\Delta} \Delta^{\dagger iA} (w_i^A N + \text{H.c.}) + \dots,
\end{aligned} \tag{1}$$

where we list only the terms pertinent to our calculation. The pion decay constant is  $f = 92.4$  MeV,  $\xi_L, \xi_R$  are  $SU(2)$  matrices parameterizing the chiral  $SU_L(2) \times SU_R(2)$  group and  $\mathcal{M} = \text{diag}(m_q, m_q)$  is the quark mass matrix in the isospin limit (the precise conventions used can be found in Appendix A). The values of the other low-energy constants will be given when we discuss our results. The Goldstone bosons belong to the coset space  $[SU_L(2) \times SU_R(2)]/SU_{L+R}(2)$ , and we are free to choose an arbitrary member to be the representative of each coset (“fix the gauge”). Instead of the usual choice  $\xi_L = \xi_R^\dagger = \xi = e^{\frac{i\pi \cdot \tau}{2f}}$ , we use the choice made in background field calculations

$$\begin{aligned}
\xi_L &= u_0 e^{\frac{i\pi \cdot \tau}{2f}}, \\
\xi_R &= u_0^\dagger e^{-\frac{i\pi \cdot \tau}{2f}},
\end{aligned} \tag{2}$$

where  $u_0$  is a space-time independent field and  $\pi(x)$  does not contain zero-modes:

$$\pi(x) = \sum_{n_\mu \neq (0, \vec{0})} \pi_n e^{i \frac{2\pi n_0}{\beta} t + i \frac{2\pi \vec{n}}{L} \cdot \vec{x}}. \tag{3}$$

The rationale to separate zero- and non-zero modes is that, as we will see below, the zero modes obey a different power counting from the non-zero ones at small volumes where chiral symmetry is partially restored. The background field  $u_0$  only appears in those terms of the action which include quark masses. This can be easily seen by noticing that a non-trivial background  $u_0$  corresponds to a chiral rotation of the vacuum one expands around. In the absence of quark masses, all such vacua are equivalent, so the physics of the Goldstone bosons is the same. The terms which do however depend on the quark masses are in the isospin limit with  $\mathcal{R}[\text{Tr}(A) = \frac{1}{2} \text{Tr}(A + A^\dagger)]$ :

$$- m_q B f^2 \mathcal{R}[\text{Tr}(u_0^2 e^{\frac{i\pi \cdot \tau}{f}})] - 4m_q B c_1 N^\dagger \mathcal{R} e \text{Tr}(u_0^2 e^{\frac{i\pi \cdot \tau}{f}}) N. \tag{4}$$

At leading order,  $m^2 = 2Bm_q$  is the pion mass in the infinite volume limit.

We can now estimate the different terms of the Lagrangean. The typical fluctuations of the non-zero modes  $\pi(x)$  are of the order  $\pi(x) \sim \epsilon$  since, for larger values of  $\pi(x)$ , the kinetic term is much larger than one and suppresses their contribution to the path integral (we can estimate the size of the kinetic term as  $1/\epsilon^4$  coming from the volume integral,  $\epsilon^2$  from the two derivatives and  $\epsilon^2$  from the pion fields). A similar argument implies  $N \sim \epsilon^{3/2}$ . However, as observed by Gasser and Leutwyler [2], the zero-mode  $u_0$  is of order  $\epsilon^0$ . We can conclude that by noticing that the coefficient of the first term of Eq.(4) is of order  $\sim m^2 f^2 \beta L^3 \sim \epsilon^0$ . Because the zero-mode is not suppressed, it has to be treated exactly. This is related to the restoration of chiral symmetry at finite temperatures and volumes. In

small boxes the zero-mode fluctuates over the whole group manifold, in contradistinction to the infinite volume limit in which the zero-mode makes only small fluctuations around a preferred vacuum direction. As shown in [2] the integration over the zero-mode can be performed as follows. The part of the partition function which contains  $u_0$  can be written as

$$\begin{aligned} Z[N, \Delta] &= \int [Du_0] \exp \left[ \int d^4x \left( \frac{m^2 f^2}{2} + 2m^2 c_1 N^\dagger(x) N(x) \right) \left( \mathcal{R}e \text{Tr}(u_0^2) \left( 1 - \frac{\pi^2}{2f^2} \right) + \frac{1}{f^2} \mathcal{R}e \text{Tr}(u^2 i \pi^A \tau^A) + \dots \right) \right] \\ &\approx \int [Du_0] e^{s \mathcal{R}e \text{Tr}(u_0^2)} \left[ 1 + \mathcal{R}e \text{Tr}(u_0^2) \left( 2m^2 c_1 \int d^4x N^\dagger N \left( 1 - \frac{\pi^2}{2f^2} \right) - \frac{m^2}{4} \int d^4x \pi^2 \right) \right] \\ &\approx X(s) \exp \left[ -\frac{X'(s)}{2X(s)} \int d^4x \left( -4m^2 c_1 N^\dagger(x) N(x) \left( 1 - \frac{\pi^2}{2f^2} \right) + \frac{m^2}{2} \pi^2 \right) \right] \end{aligned} \quad (5)$$

where we dropped higher orders in the pion-fields,  $s = B f^2 m_q \beta L^3 = m^2 f^2 \beta L^3 / 2$  and

$$X(s) = \int_{SU(2)} [Du_0^2] e^{s \mathcal{R}e \text{Tr}(u_0^2)} = \frac{I_1(2s)}{s}, \quad (6)$$

with  $I_1(x)$  a modified Bessel function. The integration over the zero-mode performed above renormalizes the nucleon mass (adding a term proportional to  $c_1$  of order  $\epsilon^4$  to it) and the pion mass (by a term of order  $\epsilon^0$ ), as well as the non-derivative couplings:

$$\begin{aligned} M &\rightarrow M - 4m^2 c_1 \frac{X'(\beta L^3 m^2 f^2 / 2)}{2X(\beta L^3 m^2 f^2 / 2)}, \\ m^2 &\rightarrow m_{\text{eff}}^2 = \underbrace{2m_q B}_{m^2} \frac{X'(\beta L^3 m^2 f^2 / 2)}{2X(\beta L^3 m^2 f^2 / 2)}. \end{aligned} \quad (7)$$

The effective pion mass is shown in Fig. 1. In the limit  $s \rightarrow \infty$ , one retrieves with  $X'(\infty)/(2X(\infty)) = 1$ , the well-known infinite-volume results. Notice that the shift of the nucleon and pion masses due to the zero modes

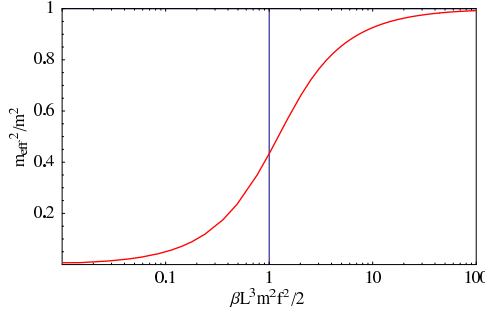


FIG. 1: The effective pion mass  $m_{\text{eff}}$  as function of  $\beta L^3 m^2 f^2 / 2$ , Eq. (7).

comes just from quenching the chiral condensate in the finite volume:

$$\frac{\langle 0 | \bar{q}q | 0 \rangle_{\beta, L}}{\langle 0 | \bar{q}q | 0 \rangle} = \frac{X'(s)}{2X(s)}. \quad (8)$$

The total partition function of the system is finally to the order considered

$$Z = \int [DN] [D\Delta] e^{-S'} Z[N, \Delta], \quad (9)$$

with  $S'$  the part of the action (1) which is independent of zero-modes.



FIG. 2: Leading-order contributions to the nucleon mass.

### NUCLEON MASS

The shift in the nucleon mass due to finite volume effects is given at leading order [ $\mathcal{O}(\epsilon^3)$ ] by the two one-loop diagrams of Fig. 2. We find for the first diagram:

$$M_a^{(3)}(\beta, L) = -\frac{3g_A^2}{4f^2} \frac{1}{\beta L^3} \sum_{n_\mu \neq 0} \frac{i}{\omega + \frac{2\pi n_0}{\beta}} \frac{(\frac{2\pi \vec{n}}{L})^2}{(\frac{2\pi n_0}{\beta})^2 + (\frac{2\pi \vec{n}}{L})^2 + m_{\text{eff}}^2} \xrightarrow{\omega \rightarrow 0} -i \frac{3g_A^2}{4f^2} \mathbb{A}(\Delta = 0, m_{\text{eff}}). \quad (10)$$

The second diagram is

$$M_b^{(3)}(\beta, L) = -\frac{4g_{N\Delta}^2}{3f^2} \sum_{n_\mu \neq 0} \frac{i}{\omega + \frac{2\pi n_0}{\beta} + i\Delta} \frac{(\frac{2\pi \vec{n}}{L})^2}{(\frac{2\pi n_0}{\beta})^2 + (\frac{2\pi \vec{n}}{L})^2 + m_{\text{eff}}^2} \xrightarrow{\omega \rightarrow 0} -i \frac{4g_{N\Delta}^2}{3f^2} \mathbb{A}(\Delta, m_{\text{eff}}). \quad (11)$$

Because  $mL, m\beta, \Delta L$  and  $\Delta\beta$  are all of order  $\epsilon$  in the  $\epsilon$  expansion, the  $m$  and  $\Delta$  contribution to these graphs are of order  $\mathcal{O}(\epsilon^5)$ , so that  $m$  (and with that of course  $m_{\text{eff}}$ ) and  $\Delta$  can be dropped from the expressions above.

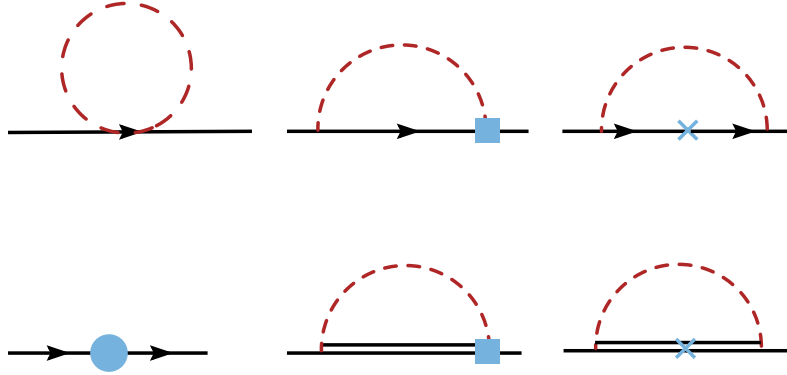


FIG. 3: Next-to-leading order diagrams for the nucleon mass. The square vertex represents a vertex suppressed by  $\epsilon$ , the cross a kinetic energy insertion, and the circle the zero-mode mass contribution. The dashed, full and double lines represent a pion, nucleon and  $\Delta$  propagator, respectively.

The first truly specific feature of the “ $\epsilon$ -régime” appears at order  $\epsilon^4$ , because the nucleon mass receives contributions from the zero modes computed above in Eq. (7) in addition to the graphs shown in Fig. 3. The first graph leads to

$$M_a^{(4)}(\beta, L) = -\frac{3\bar{c}_2 + 3c_3}{f^2} \frac{1}{\beta L^3} \sum_{n_\mu \neq 0} \frac{(\frac{2\pi n_0}{\beta})^2}{(\frac{2\pi n_0}{\beta})^2 + (\frac{2\pi \vec{n}}{L})^2 + m_{\text{eff}}^2} - \frac{3c_3}{f^2} \frac{1}{\beta L^3} \sum_{n_\mu \neq 0} \frac{(\frac{2\pi \vec{n}}{L})^2}{(\frac{2\pi n_0}{\beta})^2 + (\frac{2\pi \vec{n}}{L})^2 + m_{\text{eff}}^2} = -\frac{3\bar{c}_2 + 3c_3}{f^2} \mathbb{C}(m_{\text{eff}}) - \frac{3c_3}{f^2} \mathbb{D}(m_{\text{eff}}), \quad (12)$$

with  $\bar{c}_2 = c_2 - \frac{g_A^2}{8M}$ . The second and fifth graph vanishes. The third one gives

$$M_c^{(4)}(\beta, L) = \frac{3g_A^2}{8Mf^2} \frac{1}{\beta L^3} \sum_{n_\mu \neq 0} \left( \frac{i}{\omega + \frac{2\pi n_0}{\beta}} \right)^2 \frac{(\frac{2\pi \vec{n}}{L})^4}{(\frac{2\pi n_0}{\beta})^2 + (\frac{2\pi \vec{n}}{L})^2 + m_{\text{eff}}^2}$$

$$= -\frac{3g_A^2}{8Mf^2}\mathbb{B}(\Delta = 0, m_{\text{eff}}). \quad (13)$$

The fourth graph is the non-perturbative contribution computed before in Eq. (7) as

$$M_d^{(4)}(\beta, L) = -2m^2 c_1 \frac{X'(m^2 f^2 \beta L^3/2)}{X(m^2 f^2 \beta L^3/2)}, \quad (14)$$

and the last one contributes as

$$\begin{aligned} M_f^{(4)}(\beta, L) &= \frac{2g_{N\Delta}^2}{3Mf^2} \frac{1}{\beta L^3} \sum_{n_\mu \neq 0} \left( \frac{i}{\omega + \frac{2\pi n_0}{\beta} + i\Delta} \right)^2 \frac{(\frac{2\pi \vec{n}}{L})^4}{(\frac{2\pi n_0}{\beta})^2 + (\frac{2\pi \vec{n}}{L})^2 + m_{\text{eff}}^2} \\ &= -\frac{2g_{N\Delta}^2}{3Mf^2}\mathbb{B}(\Delta, m_{\text{eff}}). \end{aligned} \quad (15)$$

The functions  $\mathbb{A}$ ,  $\mathbb{B}$ ,  $\mathbb{C}$  and  $\mathbb{D}$  are calculated in Appendix B. We reduced them to rapidly converging sums for non-zero values of  $m_{\text{eff}}$  and  $\Delta$ , but no analytic form is available. A *Mathematica* notebook computing these functions is available from the authors' website<sup>1</sup>. In the  $\epsilon$  expansion, the contributions coming from the finite values of  $m$  and  $\Delta$  appear only at order  $\epsilon^5$  in the loop diagrams, so we should take for these  $m = \Delta = 0$  at the order  $\epsilon^4$  we are working. In this case, a simple form for the nucleon mass-shift is available:

$$\delta M^{(3+4)} = \frac{1}{f^2 L^3} \left( \frac{3g_A^2}{8} + \frac{2g_{N\Delta}^2}{3} \right) \left( 1 - \frac{\tau(\beta/L)}{ML} \right) - \frac{3\bar{c}_2}{f^2 L^4} \left( \tau(\beta/L) - \frac{L}{\beta} \right) + \frac{3c_3}{f^2 \beta L^3} - 2m^2 c_1 \left( \frac{X'(m^2 f^2 \beta L^3/2)}{X(m^2 f^2 \beta L^3/2)} - 2 \right), \quad (16)$$

where

$$\gamma_0 = \frac{1}{\pi^2} \sum_{\vec{j} \neq 0} \frac{1}{j^4} \approx 1.675, \quad \tau(x) = \frac{\gamma_0}{2} - \sum_{\vec{j} \neq 0} \frac{2\pi j}{e^{2\pi j x} - 1}, \quad (17)$$

with  $j = |\vec{j}|$ . The function  $\tau(x)$  is plotted in Fig. 4.

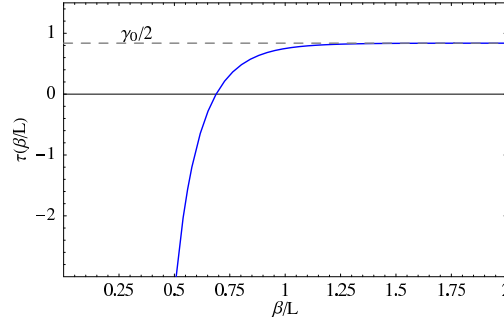


FIG. 4:  $\tau(\beta/L)$  as a function of the box asymmetry  $\beta/L$ .

For not-so-small boxes satisfying  $mL \sim \beta\Delta \gtrsim 1$ , the  $p$  expansion applies. The two leading orders in the expansion of the nucleon mass in the  $p$ -régime are very similar to the ones in the  $\epsilon$ -régime. The differences are: i) leading and next-to-leading order are switched as the quark mass insertion proportional to  $c_1$  is the leading ( $p^2$ ) order contribution while the diagrams in Fig. 2 are the next-to-leading ( $p^3$ ) contribution (terms proportional to  $c_2, c_3$  are even higher, namely  $p^4$ ); and ii) the non-zero value of  $m$  and  $\Delta$  should be kept in the diagrams. For this reason, if we keep the pion mass in our calculations, which in the  $\epsilon$ -régime is a sub-leading ( $\epsilon^5$ ) effect, our expressions will be valid in both régimes and, in particular, in the intermediate region  $(L, \beta) \cong 1/m$ . This way, they also include some, but not all  $\mathcal{O}(\epsilon^5)$  pieces<sup>2</sup>. Furthermore, since the pion mass in the  $\epsilon$ -régime has a correction of order  $\epsilon^0$  coming from the integration over the zero-mode (Eq.(7)), we use  $m_{\text{eff}}$  in the one-loop diagrams.

<sup>1</sup> <http://nta0.lbl.gov/~bedaque/index.html> or <http://ph.tum.de/~hgrie>

<sup>2</sup> Our results are also valid in the limit  $\beta \rightarrow \infty$  as long as this limit is taken at fixed  $m$ . If  $m^2\beta$  is kept fixed instead with  $s = m^2\beta f^2 L^3/2 \sim 1$ , the mass term does not prevent the ( $\vec{n} = 0, n_0 \neq 0$ ) modes to have large fluctuations and they become non-perturbative. This is the  $\delta$  régime discussed first in Ref. [4].

## EUCLIDEAN TIME AND THE CORRECT ANALYTIC CONTINUATION

There is a subtlety in computing the nucleon mass using the combination of the finite-temperature imaginary time and heavy baryon formalisms we used. To see that, consider the derivation of the heavy baryon Lagrangean. One starts from the relativistic nucleon field  $\psi$  and performs a field redefinition which reads in Euclidean space

$$\psi(\tau, \vec{r}) = e^{-M\tau}(N(\tau, \vec{r}) + H(\tau, \vec{r})), \quad (18)$$

where  $M$  is the heavy nucleon mass and  $N$  and  $H$  are the nucleon and (anti)-nucleon fields satisfying  $\gamma^0 N = N$ ,  $\gamma^0 H = -H$ . An “on-shell”  $\psi$  field has a fast variation with time ( $\partial_0 \psi \sim M$ ), while an “on-shell”  $N$  satisfies  $\partial_0 N \sim 0$ . The Lagrangean in terms of these new variables is

$$\bar{\psi}(\partial_0 \gamma_0 + M)\psi \rightarrow N^\dagger(\partial_0 + \dots)N + H^\dagger(\partial_0 - 2M + \dots)H + \dots \quad (19)$$

The “heavy” field  $H$  can then be integrated out and we are left with the usual heavy baryon Lagrangean. Notice that the anti-periodic boundary condition in the time direction for the relativistic field implies a different boundary condition for the heavy-nucleon field

$$\psi(\beta, \vec{r}) = -\psi(0, \vec{r}) \Rightarrow N(\beta, \vec{r}) = -e^{\beta M} N(0, \vec{r}). \quad (20)$$

Therefore, the field  $N$  has the Fourier decomposition

$$N(\tau, \vec{r}) = \sum_{n_0} e^{-i(\frac{\pi(2n_0+1)}{\beta} + iM)\tau} N(n_0, \vec{r}) \quad (21)$$

The correlators of the field  $N$  are defined only at shifted values of (imaginary) frequency, namely at  $\omega = \pi(2n+1)/\beta + iM$ .

Consider now, as an example, the computation of the first diagram in Fig. 2. For simplicity, we consider the infinite spatial volume limit. As shown in Appendix C, the sum over  $n$  can be performed resulting up to constants in

$$\begin{aligned} \mathcal{G}(\omega) &= \frac{1}{\beta} \sum_n \int \frac{d^3 k}{(2\pi)^3} \vec{k}^2 \frac{i}{\frac{2\pi n}{\beta} + \omega + i\Delta} \frac{1}{(\frac{2\pi n}{\beta})^2 + \omega_k^2} \\ &= \int \frac{dk^4}{(2\pi)^4} \frac{1}{k_0 + \omega + i\Delta} \frac{\vec{k}^2}{k_0^2 + \omega_k^2} - i \int \frac{dk^3}{(2\pi)^3} \frac{\vec{k}^2}{(\omega + i\Delta)^2 + \omega_k^2} \frac{1}{e^{\beta(\Delta - i\omega)} - 1} \\ &\quad + \int \frac{dk^3}{(2\pi)^3} \frac{\vec{k}^2}{(\omega + i\Delta)^2 + \omega_k^2} \frac{\omega + i\Delta}{\omega_k} \frac{1}{e^{\beta\omega_k} - 1}. \end{aligned} \quad (22)$$

where  $\omega$  is the external energy and  $\omega_k^2 = \vec{k}^2 + m^2$ . We now substitute  $\omega$  from above into the second term,

$$\frac{1}{e^{\beta(\Delta - i\omega)} - 1} = -\frac{1}{e^{\beta(M + \Delta)} + 1} \approx 0, \quad (23)$$

leading to the correct statistics for fermionic ensembles. Physically, that we neglect these fluctuations just mirrors the fact that finite-temperature fluctuations of heavy particles are much smaller than those of light ones for temperatures  $\beta M \gg 1$  at which the heavy-baryon formalism applies. Therefore, we drop this term and arrive at

$$\mathcal{G}(\omega) = \int \frac{dk^4}{(2\pi)^4} \frac{1}{k_0 + \omega + i\Delta} \frac{\vec{k}^2}{k_0^2 + \omega_k^2} + \int \frac{dk^3}{(2\pi)^3} \frac{\vec{k}^2}{(\omega + i\Delta)^2 + \omega_k^2} \frac{\omega + i\Delta}{\omega_k} \frac{1}{e^{\beta\omega_k} - 1}. \quad (24)$$

The nucleon propagator at any value of the external energy (including real values) can be obtained from the expression above by analytically continuing in  $\omega$ . In particular, the value determining the mass is obtained for  $\omega = 0$ . Clearly, this procedure seems arbitrary for two reasons. First, it seems to depend on the order between setting  $\omega$  to  $\omega = \pi(2n+1)/\beta + iM$  and analytically continuing to  $\omega = 0$ . Second, the knowledge of the propagator at discrete values of the frequency is not, in general, enough to determine the propagator on the whole complex plane. One could, for instance, have maintained  $e^{-i\beta\omega}$  instead of substituting it by  $-e^{\beta M}$  and using  $e^{-2\pi i n} = 1$ . Fortunately, the analytic continuation is unique for functions vanishing at infinity at least like  $1/|\omega|$  [5], as in the case at hand. Still, to confirm that we have picked the correct analytic continuation, we repeat this calculation in Appendix C without using the heavy baryon formalism in another method to compute finite-temperature corrections which does not require an analytic continuation to the real axis, namely the “real time formalism”.

## NUMERICAL EXAMPLES AND DISCUSSION

We now present some numerical examples in order to explore the convergence of the  $\epsilon$ -expansion and to discuss how it can be used in the one baryon sector. The leading order result depends on two low energy constants  $g_A = 1.267$  and  $g_{N\Delta}$ , as well as on the masses and mass splittings  $m$ ,  $M$  and  $\Delta$ , whose experimental values are reasonably well known. At next-to-leading order, the constants  $c_1, c_2$  and  $c_3$  appear. They are determined experimentally through the analysis of pion-nucleon scattering. As they are most sensitive to the isoscalar part of the amplitude, where different phase shift analyses disagree, large uncertainties exist in their determination.

When considering very low energy observables, as we are here, the inclusion of the  $\Delta$  as explicit degree of freedom is optional. Let us first discuss the case where the  $\Delta$  is included. In this case, a determination of the low energy constants was made by comparing calculations to the pion-nucleon phase shift data [6]. In this work, different fits were discussed using two different phase shift analyses, and also including information about the  $\sigma$ -term. The values of  $c_1$  and  $c_3$  are more stable among different fits, while  $c_2$  varies much more.

Eq.(16) shows however that for a certain value of the ratio  $\beta/L \approx 1.22262$ ,  $\tau(1.22262) = 1/1.22262$  and the dependence on  $c_2$  disappears. Since  $c_1$  and  $g_{N\Delta}$  are much better determined, one might use the mass-shifts measured around this ratio on the lattice to determine  $c_3$ . The  $c_2$ -contribution is generically negligible for  $\beta/L \sim [1 \dots 1.7]$ .

In Fig. 5, we present results using the parameter set (fit 2<sup>†</sup> of Table 4 in [6]) :

$$\begin{aligned} g_{N\Delta} &= 1.00 \pm 0.08, \\ c_1 &= -0.35 \pm 0.09/\text{GeV}, \\ c_2 &= -1.49 \pm 0.67/\text{GeV}, \\ c_3 &= 0.93 \pm 0.87/\text{GeV}. \end{aligned} \tag{25}$$

The errors quoted come from the fit and under-estimate the uncertainty in the constants from higher-order corrections. In the left panel of Fig. 5, we show the leading contribution and its next-to-leading order correction to the mass shift computed both using Eq.(16) and the full formula with finite  $m_{eff}$  and  $\Delta$ . The expansion in  $m/(4\pi f)$ ,  $\Delta/(4\pi f)$  seems to converge for the low-energy constants  $c_i$  in the given range, except for those close to the upper limit and for  $L$  smaller than about 1.5 fm, where one approaches the breakdown scale:  $L/(2\pi) \approx 1/(4\pi f)$ . The right panel displays the total mass shift up to second order for different values of  $c_3$  between the minimum and maximum values suggested by Eq.(25). We notice that the cancellation of the  $c_2$ -contribution for  $\beta = 1.22262L$  works very well even for non-zero pion masses, with its contribution to the mass shift never exceeding 5 MeV even for  $m = 300$  MeV.

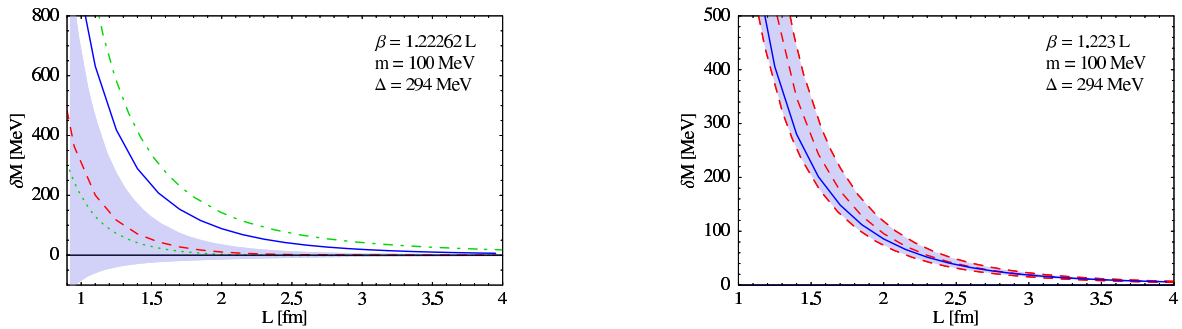


FIG. 5: Left: Finite-volume mass-shift of the nucleon in the theory with explicit  $\Delta$  degrees of freedom in MeV as function of  $L$  [fm] with the central values of the parameter set in Eq.(25). Leading order with full expansion (blue solid line); and using  $m = \Delta = 0$  Eq.(16) (green dash-dotted). Next-to-leading order *correction* in the full expansion (red dashed); and from Eq.(16) (green dotted). The gray zone shows the variation of the mass shift as  $c_3$  varies in the range given in Eq.(25), with the upper limit corresponding to  $c_3 = 1.8/\text{GeV}$ . Right: Total mass-shift at leading order (blue solid line) and at leading + next-to-leading order for  $c_3 = 0.06/\text{GeV}$ ,  $0.93/\text{GeV}$  and  $1.8/\text{GeV}$  from top to bottom (red dashed). The parameters  $\beta = 1.22262L$ ,  $m = 100$  MeV and  $\Delta = 294$  MeV are the same for both figures.

In a effective theory without explicit  $\Delta$ , its large rôle in the pion-nucleon interaction is absorbed by the couplings  $c_2$  and  $c_3$ . In fact, a simple tree level model of the  $\Delta$  contribution gives a contribution of  $c_2 = -c_3 = g_A^2 \Delta / (2(\Delta^2 - m^2)) \approx 4/\text{GeV}$ . These values are somewhat larger than what is expected from naive dimensional analysis arguments and puts the quark mass expansion in check. The values suggested by different fits

[7, 8, 9] roughly agree with the  $\Delta$  saturation estimate. We show in Fig. 6, as an example, the mass shift computed with the central values of the parameter set

$$\begin{aligned} c_1 &= -0.81 \pm 0.15/\text{GeV}, \\ c_2 &= 2.99 \pm 0.77/\text{GeV}, \\ c_3 &= -4.70 \pm 0.95/\text{GeV} \end{aligned} \quad (26)$$

advocated in [7], as well as for a somewhat smaller value of  $c_3 = -3.4/\text{GeV}$  found e.g. in the partial wave analysis of nucleon-nucleon scattering [8]. The convergence is obviously poor in either case. While the contributions from  $c_2$  and  $c_3$  can be made small for certain ratios  $\beta/L$ , this cancellation depends sensitively on the particular values chosen for  $c_2$  and  $c_3$  and is hence less useful for lattice determinations. At the ratio  $\beta/L = 1.22262$ , the  $c_2$ -contribution disappears as before, but it is already negligible at  $\beta = L$ . Indeed, a plot of the next-to-leading order correction with  $\beta/L = 1.22262$  differs from Fig. 6 at most at the 5%-level.

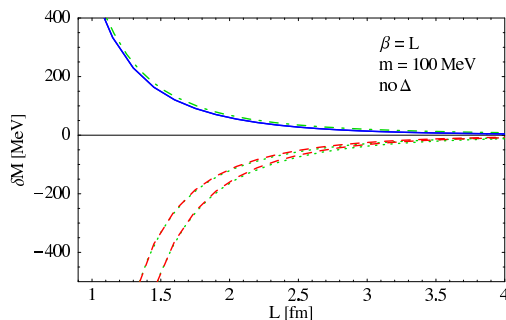


FIG. 6: Example of the finite-volume mass-shift of the nucleon at leading order (solid line) and the next-to-leading order *correction* (dashed lines) in MeV as function of  $L$  [fm] in the theory without explicit  $\Delta$  degrees of freedom. The lower dashed curve uses the central values of the parameter set in Eq.(26), the lower one changes only  $c_3 = -3.4/\text{GeV}$  following [8]. The pion mass is  $m = 100$  MeV, and  $\beta = L$ . Dot-dashed (dotted): LO (NLO) for  $m = \Delta = 0$ .

One might wonder why the expansion in the  $\epsilon$ -regime is so sensitive on the low-energy constants and converges badly in the case without  $\Delta$ , while it is well behaved in the infinite volume limit. This seems to arise because  $c_2$  and  $c_3$  appear only at third order in the  $p$ -expansion and are, consequently, poorly determined. In the  $\epsilon$ -regime, they contribute already at second order, so that the uncertainty in their values is enhanced.

## CONCLUSIONS

We have computed the nucleon mass in a finite box of size  $\beta \times L^3$  satisfying  $4\pi f \gg 2\pi/\beta, 2\pi/L \gg m$  ( $\epsilon$ -regime). Taking the value of the low energy constants suggested by experiment, we find that the expansion seems to converge for the values of the low energy constants allowed by fits made to pion-nucleon scattering data, if the  $\Delta(1232)$  is taken into account as explicit degree of freedom. We notice that a particular shape of the box ( $\beta \approx 1.22262L$ ) eliminates the dependence on one of the low energy constants ( $c_2$ ) and suggests determining the value of the most poorly known one ( $c_3$ ) by a fit to the nucleon mass with a few different box sizes. We also discussed a subtle point involving the combined use of the imaginary time and heavy baryon formalisms.

We close with the remark that it may seem strange to compute pion loops in small boxes of sizes  $\approx 1 \text{ fm}^4$ , since the momentum of the first non-zero mode  $p \approx 1.2 \text{ GeV}$  is well above the range of validity of Chiral Perturbation Theory. An alternative to our procedure that is not subject to this criticism would be to integrate out all modes but the zero-mode and obtain an effective theory which is valid only for zero-momentum observables like the mass computed here. We point out, however, that in order to connect the low-energy constants of this new theory with the parameters of the original chiral Lagrangean, one has to perform a matching calculation that is equivalent to the calculation presented in this paper.



## ACKNOWLEDGEMENTS

We would like to thank W. Detmold, Th. R. Hemmert, N. Kaiser, U.-G. Meißner and M. Savage for discussions on the topic. H.W.G. and G.R. are grateful to the Nuclear Theory Group at Lawrence Berkeley National Laboratory for warm hospitality and financial support during the first stages of this work, and H.W.G. to the Nuclear Theory Group at Los Alamos National Laboratory for the same reason. H.W.G. is supported in part by the Bundesministerium für Forschung und Technologie and by the Deutsche Forschungsgemeinschaft under contract GR1887/2-2. This work was supported in part by the U.S. Department of Energy under Contract No. DE-AC03-76SF00098 and W-7405-ENG-36.

## APPENDIX A: CONVENTIONS

We collect here the definitions used in the construction of the chiral Lagrangean. Elements of  $SU_L(2) \times SU_R(2)$  are parameterized by  $(\xi_L, \xi_R)$ .  $N$  is a spin and isospin doublet with its indices not shown explicitly.  $\Delta^{iA}$  is a spin-isospin 3/2-field, where the vector and isovector indices  $jA$  are explicitly shown, besides the implicit spin and isospin indices. In addition, it satisfies  $\sigma^i \Delta^{iA} = \tau^A \Delta^{iA} = 0$  so only 4 spin and 4 isospin entries are independent, as expected for (iso)spin 3/2 objects. The chiral transformation rules are

$$\begin{aligned}\xi_L &\rightarrow L \xi_L h^{-1}, \\ \xi_R &\rightarrow R \xi_R h^{-1}, \\ N &\rightarrow h N, \\ \Delta^{iA} &\rightarrow \underbrace{\frac{1}{2} \text{Tr}(h^{-1} \tau^A h \tau^B)}_{\mathcal{O}^{AB}} h \Delta^{iB},\end{aligned}\tag{27}$$

where  $\mathcal{O}^{AB}$  is an orthogonal matrix which is determined by  $h$  via  $h^{-1} \tau^A h = \mathcal{O}^{AB} \tau^B$ , where  $h$  in turn depends on  $\pi(x)$ ,  $L$  and  $R$ . In addition, we define some objects with simple chiral transformation rules

$$\begin{aligned}\mathcal{V}_\mu &= \frac{1}{2}(\xi_R^\dagger \partial_\mu \xi_R + \xi_L^\dagger \partial_\mu \xi_L) \rightarrow h \mathcal{V}_\mu h^{-1} + h \partial_\mu h^{-1}, \\ \mathcal{A}_\mu &= \frac{i}{2}(\xi_R^\dagger \partial_\mu \xi_R - \xi_L^\dagger \partial_\mu \xi_L) \rightarrow h \mathcal{A}_\mu h^{-1}, \\ D_\mu N &= \partial_\mu N + \mathcal{V}_\mu N \rightarrow h D_\mu N, \\ D_\mu \Delta^{iA} &= \partial_\mu \Delta^{iA} + \mathcal{V}_\mu \Delta^{iA} + i \epsilon^{ABC} \text{Tr}(\tau^B \mathcal{V}_\mu) \Delta^{iC} \rightarrow \mathcal{O}^{AB} h D_\mu \Delta^{iB}, \\ D_\mu \mathcal{A}_\nu &= \partial_\mu \mathcal{A}_\nu + [\mathcal{V}_\mu, \mathcal{A}_\nu] \rightarrow h D_\mu \mathcal{A}_\nu h^{-1}, \\ w_\mu^A &= \text{Tr}(\tau^A \mathcal{A}_\mu) \rightarrow \mathcal{O}^{AB} w_\mu^B, \\ w_{\mu\nu}^A &= \text{Tr}(\tau^A D_\mu \mathcal{A}_\nu) \rightarrow \mathcal{O}^{AB} w_{\mu\nu}^B.\end{aligned}\tag{28}$$

## APPENDIX B: CALCULATION OF SUMS

In this appendix, we drop for clarity the subscript of the effective pion mass  $m_{\text{eff}}$  and denote it by  $m$ . The LO diagrams contain then the sum

$$\begin{aligned}\mathbb{A}(\Delta, m) &= \frac{1}{\beta L^3} \sum_{n_\mu \neq 0} \frac{1}{\omega + \frac{2\pi n_0}{\beta} + i\Delta} \frac{(\frac{2\pi \vec{n}}{L})^2}{(\frac{2\pi n_0}{\beta})^2 + (\frac{2\pi \vec{n}}{L})^2 + m^2} \\ &= \mathbb{A}_0(\Delta, m) + \mathbb{A}_\beta(\Delta, m),\end{aligned}\tag{29}$$

where  $\omega = 2\pi(k + 1/2)/\beta$  is a discrete external energy and  $k$  an integer. The ultraviolet divergence of  $\mathbb{A}$  is identical to the one in the infinite-volume diagram and cancels in the difference between finite and infinite volume masses. For this cancellation to occur, it is important to use the same regulator in both calculations. In practice, we should therefore define the sum above using dimensional regularization.  $\mathbb{A}_0$  and  $\mathbb{A}_\beta$  are the temperature independent and

the finite temperature parts:

$$\begin{aligned}\mathbb{A}_0(\Delta, m) &= \int \frac{dk_0}{2\pi} \frac{1}{L^3} \sum_{\vec{n}} \frac{1}{k_0 + \omega + i\Delta} \frac{(\frac{2\pi\vec{n}}{L})^2}{k_0^2 + (\frac{2\pi\vec{n}}{L})^2 + m^2}, \\ \mathbb{A}_\beta(\Delta, m) &= \frac{i}{L^3} \sum_{\vec{n}} \frac{\Delta - i\omega}{\omega_n^2 - (\Delta - i\omega)^2} \frac{(\frac{2\pi\vec{n}}{L})^2}{\omega_n} \frac{1}{e^{\beta\omega_n} - 1} - \frac{i}{L^3} \sum_{\vec{n}} \frac{(\frac{2\pi\vec{n}}{L})^2}{\omega_n^2 - (\Delta - i\omega)^2} \frac{1}{e^{\beta(\Delta - i\omega)} - 1},\end{aligned}\quad (30)$$

where  $\omega_n^2 = \frac{2\pi\vec{n}^2}{L} + m^2$ . We used the formula

$$\frac{1}{\beta} \sum_n f\left(\frac{2\pi n}{\beta}\right) = \int_{-\infty}^{\infty} \frac{dz}{2\pi} f(z) - i\text{Res}\left(\frac{f(z)}{e^{i\beta z} - 1}\right)|_{\text{lowerplane}} + i\text{Res}\left(\frac{f(z)}{e^{-i\beta z} - 1}\right)|_{\text{upperplane}}, \quad (31)$$

which holds if  $f(z)$  has no poles on the real axis. We substitute  $1/(e^{\beta(\Delta - i\omega)} - 1)$  by  $-1/(e^{\beta(\Delta + M)} + 1) \approx 0$  as in Eq. (23). The zero-temperature part can be computed with the help of the relation [10]

$$\begin{aligned}\frac{1}{L^3} \sum_{\vec{n}} \frac{(\frac{2\pi\vec{n}}{L})^{2m}}{(\frac{2\pi\vec{n}}{L})^2 + x^2} &= \frac{1}{L^3} \int d^3k \frac{k^{2m}}{k^2 + x^2} \sum_{\vec{n}} \delta\left(\vec{k} - \frac{2\pi\vec{n}}{L}\right) = \int \frac{d^3k}{(2\pi)^3} \frac{k^{2m}}{k^2 + x^2} \underbrace{\sum_{\vec{n}} \delta\left(\frac{\vec{k}L}{2\pi} - \vec{n}\right)}_{\sum_{\vec{j}} e^{iL\vec{k}\cdot\vec{j}}} \\ &= \int \frac{d^3k}{(2\pi)^3} \frac{k^{2m}}{k^2 + x^2} + \int \frac{d^3k}{(2\pi)^3} \sum_{\vec{j} \neq 0} \frac{k^{2m}}{k^2 + x^2} e^{iL\vec{k}\cdot\vec{j}} \\ &= \int \frac{d^3k}{(2\pi)^3} \frac{k^{2m}}{k^2 + x^2} + \sum_{\vec{j} \neq 0} \frac{1}{2\pi^2 L} \int_0^\infty dk \frac{k^{(2m+1)} \sin(jkL)}{j} \\ &= \int \frac{d^3k}{(2\pi)^3} \frac{k^{2m}}{k^2 + x^2} + \frac{(-x^2)^m}{4\pi L} \sum_{\vec{j} \neq 0} \frac{e^{-jxL}}{j},\end{aligned}\quad (32)$$

where  $m$  is a positive integer. Applying this relation to  $\mathbb{A}_0$  yields

$$\delta\mathbb{A}_0 = \mathbb{A}_0 - \mathbb{A}(\beta \rightarrow \infty, L \rightarrow \infty) = \frac{i\Delta^2}{4\pi^2 L} \sum_{\vec{j} \neq 0} \frac{1}{j} \underbrace{\frac{1}{\Delta} \int_0^\infty dk_0 \frac{k_0^2 + m^2}{k_0^2 + \Delta^2} e^{-jL\sqrt{k_0^2 + m^2}}}_{g(jL, m, \Delta)}. \quad (33)$$

Asymptotically, the sum over  $j$  converges because

$$\begin{aligned}g(jL, m, \Delta) &\xrightarrow{j \rightarrow \infty} \frac{m^{5/2}}{\Delta^3} \sqrt{\frac{\pi}{2jL}} e^{-jmL} + \dots, \\ g(jL, 0, \Delta) &\xrightarrow{j \rightarrow \infty} \frac{2}{j^3 L^3 \Delta^3} + \dots.\end{aligned}\quad (34)$$

These asymptotic forms are also useful in the numerical evaluation of the sum over  $\vec{j}$ .

We also need  $\mathbb{A}_0$  evaluated at  $\Delta = 0$ . We can obtain this limit noticing that the integral defining  $g(jL, m, \Delta)$  is nearly infrared divergent when  $\Delta \rightarrow 0$ , and hence is dominated by small values of  $k_0$ . The  $\Delta \rightarrow 0$  limit of  $g(jL, m, \Delta)$  is given by

$$g(jL, m, \Delta) \xrightarrow{\Delta \rightarrow 0} \frac{1}{\Delta} \int_0^\infty dk_0 \frac{k_0^2 + m^2}{k_0^2 + \Delta^2} e^{-jmL - jL\frac{k_0^2}{2m}} = \frac{\pi}{2} \frac{m^2}{\Delta^2} e^{-jmL}. \quad (35)$$

Using this result,

$$\delta\mathbb{A}_0(\Delta = 0, m) = \frac{im^2}{8\pi L} \sum_{\vec{j} \neq 0} \frac{e^{-jmL}}{j}. \quad (36)$$

The expression above agrees with that of Ref. [1]. The limit  $m \rightarrow 0$  is found by noticing that for small values of  $m$ , the sum is dominated by the large  $j$  terms, which in turn can be approximated by an integral

$$\delta\mathbb{A}_0(\Delta = 0, m) \xrightarrow{m \rightarrow 0} \frac{im^2}{8\pi L} 4\pi \int_0^\infty j e^{-jmL} \xrightarrow{m \rightarrow 0} \frac{i}{2L^3}. \quad (37)$$

The double limit  $\Delta \rightarrow 0, m \rightarrow 0$  can also be obtained in the opposite order, and the result is the same:

$$\begin{aligned} \delta\mathbb{A}_0(\Delta, m = 0) &= \frac{i}{4\pi^2 L} \sum_{j \neq 0} \frac{1}{j} \Delta \int_0^\infty dk_0 \frac{k_0^2}{k_0^2 + \Delta^2} e^{-jLk_0} \\ &= \frac{i\Delta^2}{4\pi^2 L} \sum_{j \neq 0} \frac{1}{j} \underbrace{\left[ \frac{1}{jL\Delta} - Ci(jL\Delta) \sin(jL\Delta) + Si(jL\Delta) \cos(jL\Delta) - \frac{\pi}{2} \cos(jL\Delta) \right]}_{g(jL, 0, \Delta)} \\ &\xrightarrow{\Delta \rightarrow 0} \frac{i\Delta^2}{4\pi^2 L} 4\pi \underbrace{\int_0^\infty dj j g(jL, 0, \Delta)}_{\frac{\pi}{2L^2\Delta^2}} = \frac{i}{2L^3} \end{aligned} \quad (38)$$

The finite-temperature part converges very quickly:

$$\begin{aligned} \mathbb{A}_\beta &= \frac{i}{L^3} \sum_{\vec{n}} \frac{\Delta}{\omega_n^2 - \Delta^2} \frac{(\frac{2\pi\vec{n}}{L})^2}{\omega_n} \frac{1}{e^{\beta\omega_n} - 1} \\ &\xrightarrow{\Delta \rightarrow 0} 0. \end{aligned} \quad (39)$$

The second sum we need is

$$\mathbb{B}(\Delta, m) = \frac{1}{\beta L^3} \sum_{n_\mu \neq 0} \left( \frac{1}{\frac{2\pi n_0}{\beta} + i\Delta} \right)^2 \frac{(\frac{2\pi\vec{n}}{L})^4}{(\frac{2\pi n_0}{\beta})^2 + (\frac{2\pi\vec{n}}{L})^2 + m^2}. \quad (40)$$

We use Eq.(31) to separate it into a temperature-independent ( $\mathbb{B}_0$ ) and a temperature-dependent part ( $\mathbb{B}_\beta$ ). The first one is with Eq. (32)

$$\mathbb{B}_0 = \int \frac{d^4 k}{(2\pi)^4} \frac{1}{(k_0 + i\Delta)^2} \frac{\vec{k}^4}{k_0^2 + \vec{k}^2 + m^2} + \frac{1}{\pi^2 L} \sum_{j \neq 0} \frac{1}{j} \int \frac{dk_0}{2\pi} \frac{1}{(k_0 + i\Delta)^2} \int_0^\infty dk \frac{k^{5-\epsilon}}{k_0^2 + k^2 + m^2} \sin(jkL), \quad (41)$$

$$\delta\mathbb{B}_0 = \mathbb{B}_0 - \mathbb{B}(\beta \rightarrow \infty, L \rightarrow \infty) = \frac{1}{4\pi^2 L} \sum_{j \neq 0} \frac{1}{j} \underbrace{\int_0^\infty dk_0 \frac{k_0^2 - \Delta^2}{(k_0^2 + \Delta^2)^2} (k_0^2 + m^2)^2 e^{-jL\sqrt{k_0^2 + m^2}}}_{\Delta^3 h(jL, m, \Delta)}. \quad (42)$$

The sums over  $j$  converge, given the asymptotic behaviors

$$\begin{aligned} h(jL, m, \Delta) &\xrightarrow{j \rightarrow \infty} \frac{\sqrt{\pi m}}{4(jL)^{3/2}} \frac{e^{-jmL}}{\Delta^3} (m + jL(\Delta^2 - 2m^2)), \\ h(jL, m, 0) &\xrightarrow{j \rightarrow \infty} -\frac{12}{j^5 L^5 \Delta^5} + \dots \end{aligned} \quad (43)$$

Eq.(43) can be obtained from the integral representation above noticing that, for large  $j$ , the integral is dominated by small values of  $k_0$ . These relations show that the sum in Eq.(42) converges (quickly).

We also need the value of  $\delta\mathbb{B}$  at  $\Delta = 0$ , where  $h(j, L, m, \Delta)$  is *apparently* infrared divergent, but this limit is actually finite. It is most easily obtained by continuing the  $k_0$  integral to  $1 + \epsilon$  dimensions and taking the  $\epsilon \rightarrow 0$  limit at the end, with  $K_n$  again a modified Bessel function:

$$\delta\mathbb{B}_0(\Delta = 0, m) = \frac{1}{4\pi^2 L} \sum_{j \neq 0} \frac{1}{j} \int_0^\infty d^{1+\epsilon} k_0 \frac{(k_0^2 + m^2)^2}{k_0^2} e^{-jL\sqrt{k_0^2 + m^2}}$$

$$\begin{aligned}
&= \frac{m^3}{4\pi^2 L} \sum_{\vec{j} \neq 0} \frac{1}{j} \int_1^\infty dx \frac{x^5}{(x^2 - 1)^{\frac{3-\epsilon}{2}}} e^{-jLmx} \\
&= \frac{m^3}{4\pi^2 L} \sum_{\vec{j} \neq 0} \frac{1}{j} \frac{\partial^4}{\partial (jLm)^4} \int_1^\infty dx \frac{x}{(x^2 - 1)^{\frac{3-\epsilon}{2}}} e^{-jLmx} \\
&= \frac{m}{4\pi^2 L^3} \sum_{\vec{j} \neq 0} \frac{1}{j^3} [(jLm - (jLm)^3)K_0(jLm) + 2(1 + (jLm)^2)K_1(jLm)] \quad , \quad (44)
\end{aligned}$$

We can further take the limit  $m \rightarrow 0$ :

$$\delta\mathbb{B}_0(\Delta = 0, m \rightarrow 0) = \frac{1}{2\pi^2 L^4} \sum_{\vec{j} \neq 0} \frac{1}{j^4} = \frac{\gamma_0}{2L^4}. \quad (45)$$

To take the double limit in the opposite order leads – not surprisingly – to the same result:

$$\begin{aligned}
\delta\mathbb{B}_0(\Delta, m = 0) &= \frac{1}{4\pi^2 L} \sum_{\vec{j} \neq 0} \frac{1}{j} \underbrace{\int_0^\infty dk_0 k_0^4 \frac{k_0^2 - \Delta^2}{(k_0^2 + \Delta^2)^2} e^{-jL|k_0|}}_{\Delta^3 h(jL, 0, \Delta)} \\
&= \frac{\Delta^3}{8\pi^2 L} \sum_{\vec{j} \neq 0} \frac{1}{j} \left[ \frac{4 - 6(jL\Delta)^2}{(jL\Delta)^3} + 2Ci(jL\Delta) [jL\Delta \cos(jL\Delta) + 4 \sin(jL\Delta)] \right. \\
&\quad \left. + 2Si(jL\Delta) [jL\Delta \sin(jL\Delta) - 4 \cos(jL\Delta)] \right] \\
&\xrightarrow{\Delta \rightarrow 0} \frac{1}{2\pi^2 L^4} \sum_{\vec{j} \neq 0} \frac{1}{j^4} = \frac{\gamma_0}{2L^4}. \quad (46)
\end{aligned}$$

After performing the correct analytic continuation, the temperature-dependent part  $\mathbb{B}_\beta$  is

$$\mathbb{B}_\beta = -\frac{1}{L^3} \sum_{\vec{n}} \frac{\omega_n^2 + \Delta^2}{(\omega_n^2 - \Delta^2)^2} \frac{(\frac{2\pi\vec{n}}{L})^4}{\omega_n} \frac{1}{e^{\beta\omega_n} - 1}. \quad (47)$$

Finally, we use similar steps for  $\mathbb{C}$  and  $\mathbb{D}$ :

$$\begin{aligned}
\mathbb{C}(m) &= \frac{1}{\beta L^3} \sum_{n_\mu \neq 0} \frac{(2\pi n_0/\beta)^2}{(2\pi n_0/\beta)^2 + (2\pi\vec{n}/L)^2 + m^2} \\
&= \int \frac{d^4 k}{(2\pi)^4} \frac{k_0^2}{k_0^2 + \vec{k}^2 + m^2} + \frac{m^2}{(2\pi)^2 L^2} \sum_{\vec{j} \neq 0} \frac{K_2(jmL)}{j^2} - \frac{1}{L^3} \sum_{\vec{n}} \frac{\omega_n}{e^{\beta\omega_n} - 1} \quad . \quad (48)
\end{aligned}$$

$$\begin{aligned}
\mathbb{D}(m) &= \frac{1}{\beta L^3} \sum_{n_\mu \neq 0} \frac{(2\pi\vec{n}/L)^2}{(2\pi n_0/\beta)^2 + (2\pi\vec{n}/L)^2 + m^2} \\
&= \int \frac{d^4 k}{(2\pi)^4} \frac{\vec{k}^2}{k_0^2 + \vec{k}^2 + m^2} - \frac{m^3}{(2\pi)^2 L} \sum_{\vec{j} \neq 0} \frac{1}{j} \left( K_1(jmL) + \frac{K_2(jmL)}{jmL} \right) + \frac{1}{L^3} \sum_{\vec{n}} \frac{(\frac{2\pi\vec{n}}{L})^2}{\omega_n} \frac{1}{e^{\beta\omega_n} - 1} \quad , \quad (49)
\end{aligned}$$

For  $m \rightarrow 0$ , one has to be careful with the mode  $\vec{n} = 0$ :

$$\begin{aligned}
\mathbb{C}(m = 0) &= \frac{\gamma_0}{2L^4} - \frac{1}{L^4} \sum_{\vec{n} \neq 0} \frac{2\pi n}{e^{2\pi\frac{\beta}{L}n} - 1} - \frac{1}{\beta L^3} = \frac{\tau(\beta/L)}{L^4} - \frac{1}{\beta L^3} \\
\mathbb{D}(m = 0) &= -\frac{\gamma_0}{2L^4} + \frac{1}{L^4} \sum_{\vec{n} \neq 0} \frac{2\pi n}{e^{2\pi\frac{\beta}{L}n} - 1} = -\frac{\tau(\beta/L)}{L^4}. \quad (50)
\end{aligned}$$

### APPENDIX C: RELATIVISTIC CALCULATION, REAL TIME FORMALISM AND THE CORRECT ANALYTIC CONTINUATION

In order to verify our procedure to compute the finite temperature corrections of the nucleon mass, we now repeat the calculation of the simplest diagram by dispensing of the simplifications due to the use of both the heavy-baryon and the imaginary time formalisms, followed by analytic continuation to the real axis.

The *real-time* finite temperature formalism (RTF) is another way of (perturbatively) computing finite-temperature corrections. As opposed to the more common *imaginary-time* formalism (ITF), it computes correlators directly in real time and continuous frequencies. The Feynman rules are very similar to the ones at zero temperature, except that the propagators contain an additional term describing the influence of the thermal medium on the propagation of the particles<sup>3</sup>. The pion propagator becomes

$$iD(k) = \frac{i}{k_0^2 - \vec{k}^2 - m^2 + i0} + 2\pi n_B(|k_0|)\delta(k_0^2 - \vec{k}^2 - m^2), \quad (51)$$

where  $n_B(|k_0|) = (e^{\beta|k_0|} - 1)^{-1}$  is the bosonic distribution function. The fermion propagator is

$$\begin{aligned} iS(p) &= (ip_\mu \gamma^\mu + M) \left( \frac{1}{p_0^2 - \vec{p}^2 - M^2 + i0} - 2\pi n_F(|p_0|)\delta(p_0^2 - \vec{p}^2 - M^2) \right) \\ &\stackrel{p_0 \rightarrow M+k_0, \vec{p} \rightarrow \vec{k}}{\cong} \frac{i}{k_0 + i0} - 2\pi n_F(|M+k_0|)\delta(k_0), \end{aligned} \quad (52)$$

where  $n_F(k_0) = (e^{|k_0|} + 1)^{-1}$  is the Fermi distribution function. The physical origin of these extra terms is the Pauli blocking (in the case of fermions) or stimulated emission (in the boson case) caused by the real, on-shell particles present in the medium. In the fermionic case, for instance, a state that is fully occupied ( $n_F = 1$ ) reverts the sign of the “ $i\epsilon$ ” prescription and the fermion can propagate as a hole. Notice that the number density of particles in the heavy baryon propagator is  $n_F(|M+k_0|)$  (as opposed to  $n_F(|k_0|)$ ) and therefore exponentially small at all temperatures  $\beta M \gg 1$  where the effective theory applies. As an example, let us compute the real part of the second diagram in Fig. 2, for notational simplicity in the infinite volume. Up to irrelevant constants,

$$\begin{aligned} iG(E) &= \int \frac{d^4 k}{(2\pi)^4} \vec{k}^2 ((E+k_0)\gamma^0 - \vec{k} \cdot \vec{\gamma} + M_\Delta) \left[ \frac{i}{k_0^2 - \vec{k}^2 - m^2 + i0} + 2\pi n_B(|k_0|)\delta(k_0^2 - \vec{k}^2 - m^2) \right] \\ &\quad \left[ \frac{1}{(E+k_0)^2 - \vec{k}^2 - M_\Delta^2 + i0} + 2i\pi n_F(E+k_0)\delta((E+k_0)^2 - \vec{k}^2 - M_\Delta^2) \right]. \end{aligned} \quad (53)$$

Using the relation

$$\frac{1}{x+i0} = \mathcal{P} \left( \frac{1}{x} \right) - i\pi\delta(x), \quad (54)$$

where  $\mathcal{P}$  stands for the principal value, the real part of  $G(\omega)$  is

$$\begin{aligned} \text{Re}G(\omega) &= \int \frac{d^3 k}{(2\pi)^3} \vec{k}^2 \left[ \frac{1+2n_B(\omega_k)}{2\omega_k} \left( \frac{(E+\omega_k)\gamma^0 - \vec{k} \cdot \vec{\gamma} + M_\Delta}{(E+\omega_k)^2 - \vec{k}^2 - M_\Delta^2} + \frac{(E-\omega_k)\gamma^0 - \vec{k} \cdot \vec{\gamma} + M_\Delta}{(E-\omega_k)^2 - \vec{k}^2 - M_\Delta^2} \right) \right. \\ &\quad \left. + \frac{1-2n_F(\sqrt{\vec{k}^2 + M_\Delta^2})}{2\sqrt{\vec{k}^2 + M_\Delta^2}} \left( -i\sqrt{\vec{k}^2 + M_\Delta^2}\gamma^0 - i\vec{k} \cdot \vec{\gamma} + M_\Delta \right) \right. \\ &\quad \left. \times \left( \frac{1}{(-E+\sqrt{\vec{k}^2 + M_\Delta^2})^2 - \omega_k^2} + \frac{1}{(E+\sqrt{\vec{k}^2 + M_\Delta^2})^2 - \omega_k^2} \right) \right] \\ &\stackrel{E=M+\omega}{\approx} \int \frac{d^3 k}{(2\pi)^3} \vec{k}^2 \mathcal{P} \left( \frac{1}{(\Delta-\omega)^2 - \omega_k^2} \right) \left( \frac{\omega-\Delta}{2\omega_k} (1+2n_B(\omega_k)) + \frac{1-2n_F(M+\Delta-\omega)}{2} \right). \end{aligned} \quad (55)$$

---

<sup>3</sup> In diagrams with more than one loop, the RTF rules are a little more involved.

This last result can also be obtained directly using the RTF with the heavy baryon propagator in Eq.(52).

On the other hand, we compute a related quantity, namely the Euclidean time Matsubara function  $\mathcal{G}(\omega)$  defined for discrete imaginary values of  $E = -i\pi(2n+1)/\beta$ , as

$$\begin{aligned}
\text{Re}\mathcal{G}(E) &= \frac{1}{\beta} \int \frac{d^3k}{(2\pi)^3} \vec{k}^2 \frac{-i(E + \omega_n)\gamma^0 - i\vec{k} \cdot \vec{\gamma}^2 + M_\Delta}{(E + \omega_n)^2 + \vec{k}^2 + M_\Delta^2} \frac{1}{\omega_n^2 + \omega_k^2} \\
&= \int \frac{d^4k}{(2\pi)^4} \vec{k}^2 \frac{-i(E + k_0)\gamma^0 - i\vec{k} \cdot \vec{\gamma}^2 + M_\Delta}{(E + k_0)^2 + \vec{k}^2 + M_\Delta^2} \frac{1}{k_0^2 + \omega_k^2} \\
&\quad - \int \frac{d^3k}{(2\pi)^3} \vec{k}^2 \frac{n_B(\omega_k)}{2\omega_k} \left[ \frac{-i(E + i\omega_k)\gamma^0 - i\vec{k} \cdot \vec{\gamma}^2 + M_\Delta}{(E + i\omega_k)^2 + \vec{k}^2 + M_\Delta^2} + \frac{-i(E - i\omega_k)\gamma^0 - i\vec{k} \cdot \vec{\gamma}^2 + M_\Delta}{(E - i\omega_k)^2 + \vec{k}^2 + M_\Delta^2} \right] \\
&\quad - \int \frac{d^3k}{(2\pi)^3} \vec{k}^2 \frac{1}{2\sqrt{\vec{k}^2 + M_\Delta^2}} \left[ \frac{i\sqrt{\vec{k}^2 + M_\Delta^2}\gamma^0 - i\vec{k} \cdot \vec{\gamma}^2 + M_\Delta}{(-E + i\sqrt{\vec{k}^2 + M_\Delta^2})^2 + \omega^2} \frac{1}{e^{\beta\sqrt{\vec{k}^2 + M_\Delta^2} + i\beta E} - 1} \right. \\
&\quad \left. + \frac{-i\sqrt{\vec{k}^2 + M_\Delta^2}\gamma^0 - i\vec{k} \cdot \vec{\gamma}^2 + M_\Delta}{(E + i\sqrt{\vec{k}^2 + M_\Delta^2})^2 + \omega^2} \frac{1}{e^{\beta\sqrt{\vec{k}^2 + M_\Delta^2} - i\beta E} - 1} \right] \quad (56)
\end{aligned}$$

We now substitute again  $e^{\pm i\beta E}$  by  $-1$ . The real part of  $G(E)$  is related to the Matsubara function  $\mathcal{G}(\omega)$  by analytic continuation:  $G(E) = -\mathcal{G}(-iE + 0)$  [5]. The direct calculation of  $G(E)$  using the RTF and the indirect one through analytic continuation from the ITF agree, and they also reproduce in the limit  $M \rightarrow \infty$  the calculation using both the ITF and the heavy baryon formalism discussed in the main text and in Appendix B.

- 
- [1] S. R. Beane, [arXiv:hep-lat/0403015], S. R. Beane and M. J. Savage, [arXiv:hep-ph/0404131], M. Procura, T. R. Hemmert and W. Weise, Phys. Rev. D **69**, 034505 (2004) [arXiv:hep-lat/0309020], A. Ali Khan *et al*, [arXiv:hep-lat/0312030].
  - [2] J. Gasser and H. Leutwyler, Phys. Lett. B **188**, 477 (1987).
  - [3] L. Giusti, P. Hernandez, M. Laine, P. Weisz and H. Wittig, JHEP **0404**, 013 (2004) [arXiv:hep-lat/0402002], L. Giusti, P. Hernandez, M. Laine, P. Weisz and H. Wittig, JHEP **0401**, 003 (2004) [arXiv:hep-lat/0312012], P. Hernandez and M. Laine, JHEP **0301**, 063 (2003) [arXiv:hep-lat/0212014], W. Bietenholz, T. Chiarappa, K. Jansen, K. I. Nagai and S. Shcheredin, JHEP **0402**, 023 (2004) [arXiv:hep-lat/0311012],
  - [4] H. Leutwyler, Phys. Lett. **B189**, 197 (1987).
  - [5] Abrikosov, Gorkov and Dzyaloshinski, Methods of Quantum Field Theory in Statistical Mechanis, Dover, 1975.
  - [6] N. Fettes and U. G. Meißner, Nucl. Phys. A **679** (2001), 629 [arXiv:hep-ph/0006299].
  - [7] P. Büttiker and U. G. Meißner, Nucl. Phys. A **668** (2000) 97 [arXiv:hep-ph/9908247].
  - [8] M. C. M. Rentmeester, R. G. E. Timmermans and J. J. de Swart, Phys. Rev. C **67** (2003) 044001 [arXiv:nucl-th/0302080].
  - [9] N. Fettes, U. G. Meißner and S. Steininger, Nucl. Phys. A **640** (1998) 199 [arXiv:hep-ph/9803266].
  - [10] E. Elizalde, Comm. Math. Phys. **198**, 83 (1998).